OPEN ACCESS
Journal of Innovative Optical Health Sciences
Vol. 16, No. 5 (2023) 2241001 (11 pages)

DOI: 10.1142/S1793545822410012

World Scientific
www.worldscientific.com

Rapid and efficient characterization of cervical collagen orientation using linearly polarized colposcopic images

Cat Phan Ngoc Khuong*, Dung Nguyen Huu Quang*, Hai Pham Thanh†, Long Nguyen†, Quynh Nguyen Ngoc‡, Duc Le Huynh§, Tien Tran Van*,¶ and Tu Ly Anh*

*Department of Applied Physics
Ho Chi Minh City University of Technology
268 Ly Thuong Kiet Street, District 10
Ho Chi Minh City 700 000, Vietnam

†Quality Management Department, Tu Du Hospital
284 Cong Quynh, District 1
Ho Chi Minh City 700 000, Vietnam

‡Department of Biomedical Engineering
Nguyen Tat Thanh University, 300A Nguyen Tat Thanh
District 4, Ho Chi Minh City 700 000, Vietnam

§Faculty of Science and Technology
Jean Monnet University, 11 Rue du Docteur Annino
Saint Etienne 42000, France
¶tranvantien@hcmut.edu.vn

Received 10 January 2022
Accepted 10 March 2022
Published 13 April 2022

Collagen provides tissue strength and structural integrity. Quantification of the orientated dispersion of collagen fibers is an important factor when studying the mechanical properties of the cervix. In this study, for the first time, a new method for rapid characterization of the collagen fiber orientations of the cervix using linearly polarized light colposcopy is presented. A total of 24 colposcopic images were captured using a cross-polarized imaging system with white LED light sources. In the preprocessing stage, the Red channel of the RGB image was chosen, which contains no information of the blood vessels because of the low-absorption of blood cells in the red region. OrientationJ, which is an ImageJ plug-in, was used to estimate the local orientation of the collagen fibers. The result shows that in the nonpregnant cervix, the middle zone (Zone 2) has circumferentially aligned collagen fibers while the inner zone (Zone 1) has randomly arranged. The collagen fiber dispersion in Zone 2 is much smaller than that in Zone 1 at all four quadrants region (anterior, posterior, left, and right quadrant). This new analysis technique could potentially combine with diagnostic tools to provide a quantitative platform of collagen fibers in the clinic.

Keywords: Cervix; collagen fibers; collagen orientation; coherency; cross-polarized imaging; colposcopy.

¶Corresponding author.

1. Introduction

The cervix, which is dominated by fibrous connective tissue, is primarily composed of an extracellular matrix (ECM) of collagen. Collagen – the primary component of an extracellular matrix plays an important role in increasing the biomechanical strength of the cervix. Therefore, the ultrastructure of the collagen fiber network is an important factor in studying the mechanical properties of the cervix. Determining the characterization of collagen fibers such as collagen concentration, distribution of collagen types, the amount and types of collagen cross-links, especially the orientation of collagen fibers is necessary to help the diagnosis of cervical cancer as well as preterm birth.[1–4]

In the anatomical position, the cervix is the lower fibromuscular portion of the uterus, divided into two main parts: The endocervix and the ectocervix. The endocervix is the inner part of the cervix lining the canal leading into the uterus, while the ectocervix is the portion of the cervix that bulges into the top of the vagina.[5] The changes in structural and mechanical properties of the cervix mainly relate to the organization and alignment of its hierarchical collagen fiber network. Various diagnostic imaging techniques including X-rays, second-harmonic generation (SHG), optical coherence tomography (OCT), Mueller matrix polarimetry (MMP), etc., have been used to determine the collagen fiber orientation and dispersion in the cervix.[6–11] X-rays diffraction studies show that the cervix, which is roughly cylindrical, has three anatomic regions with distinct collagen fibers orientation. In the inner and outer zones, collagen fibers are arranged parallel to the canal. In the middle zone, the collagen fibers have a preferred orientation in a circumferential around the canal.[6] Further studies on nonpregnant human cervical tissue using OCT have verified that collagen fibers in a middle zone are oriented circumferentially around the endocervical canal. These studies highlight that collagen fibers in the anterior (A) and posterior (P) quadrants are less dispersed than the left (L) and right (R) quadrants.[8] Imaging with SHG signals has emerged as a useful tool to evaluate cervical collagen fiber distribution and enables the 3D analysis of collagen architecture at the micron level. Some researches demonstrated that SHG imaging, which is suitable for the development of new *in vivo* diagnostic devices, has the potential to distinguish abnormal cervical remodeling and its disorders.[9,10] Previous studies using SHG imaging show that the primary alignment of collagen fibers is longitudinal in the region nearest the canal, and circumferentially orientated fibers appear in the central region of the cervix. At the micrometer length scale (SHG scale), the collagen fibers in Region 1 (the anterior and posterior quadrants), on average, have a similar degree of alignment compared to those in Region 2 (the left and right quadrants).[9] MMP is commonly used in biomedical imaging that enables to provide the changes in the structure of tissue with a wide field image. In previous studies, MMP was used to provide useful information in cervical pre-cancer detection relies on polarimetric images of Depolarization, Retardance, and Azimuth.[12,13] MMP has also been used extensively to measure collagen arrangement and distribution non-invasively.[11] Recently, a new low-cost snapshot MMP capable of the fast acquisition of a full Mueller matrix was developed and tested successfully on the healthy human cervix. However, further studies are necessary to evaluate the diagnostic performance of this method.[14]

In this case study, we propose a new method for low-cost and real-time to determine collagen fiber orientation distribution and dispersion across four quadrants in the cervix. First, we developed a cross-polarized imaging system based on a standard colposcope. The use of crossed polarizers in the colposcopic image eliminates glares and specular highlights in the surface as well as imaging deeper into the tissue volume.[15,16] Normally, when the emitted light penetrates the subsurface of the cervix, the blood vessels are the main cause of light absorption. The Green channel provides the best contrast of the blood vessels due to the high absorption of hemoglobin in green wavelengths. By contrast, the Red channel is not affected by the blood vessels and provides more useful information about collagen.[17] Therefore, the Red channel is preferred for further operations in the collagen orientation estimation. In imaging processing, an adaptive dual threshold with a 3×3 median filter was applied to remove speckle noise that causes a shift in the orientation value. Then, collagen fibers orientation was represented by vector field map, in which each vector has the same dimension with collagen fibers in a sub-region. We used this map to calculate the maximum angular of the region of

interest (ROI) using OrientationJ (an ImageJ-plug-in). Finally, the coherency coefficient ranging from 0 to 1 was used to indicate the degree of collagen fiber alignment.[18–20] We observe a preferred circumferential distribution of the collagen fiber in Zone 2 and randomly arranged in Zone 1.

2. Materials and Methods

2.1. *Cross-polarized colposcope design*

A traditional optical colposcope was upgraded with an auto-focusing full HD CMOS camera (Amscope, USA) (Fig. 1). Still, images can be saved in 1920 × 1080 pixels (2 mega-pixels) and motion HD video can be captured in 1080 p. The autofocus camera has an objective lens (L1) with an 18–35 mm focal length and working distance from infinite to 200 mm. The camera is connected to the computer via DarkCrystal HD Capture CD311 (AverMedia, Taiwan). For the light source (LS), we used a cool white LED (Cree XLamp@ XP-G2, China) combined with an aspheric lens (L2) to achieve uniform light distribution in the regions of interest. Imaging of the morphological and functional state of tissues may be provided based on spectral analysis of the backscattering light. Polarization-sensitive techniques for imaging were applied to eliminate specular reflection on the surface of the tissue. In this case, the first polarizer (P1) was placed in the front of the light source and the second polarizer (Edmund Optics, USA) (P2) was placed in the front of the camera to select light either parallel to or perpendicular to the incident light. The second polarizer is perpendicular to the first filter (Cross-Polarization mode - CP) for eliminating the specular reflection of light by the surface.

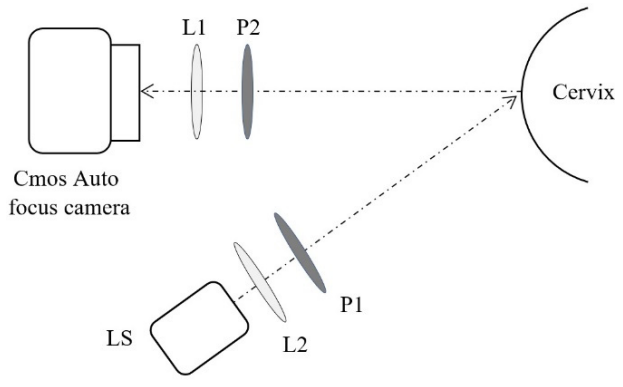

Fig. 1. Polarized light colposcopy imaging system.

2.2. *Samples*

The study was approved by the Institutional Review Board of the Vietnam National University, Ho Chi Minh City, and conducted according to the tenets of the Declaration of Helsinki. During the study period, 24 nonpregnant colposcopic images were used to determine the collagen fiber orientation distribution and dispersion of cervical tissue (Table 1). In this research, we only used images of the healthy or inflammatory cervices. Ectopy, polyp, cervical dysplasia, pre-invasive cervical disease, cervical intraepithelial neoplasia, were eliminated before starting the analysis.

In Fig. 2(a), a case of normal cervix imaging was captured using polarized light colposcopy that removes the specular reflection of light on the surface. The vagina (1) is out of focus while the ectocervix (2) is seen surrounding the cervical os (3). At the millimeter and micrometer scale, previous studies indicated that the normal cervix has three zones of preferentially aligned collagen: Collagen fibers preferentially arranged parallel to the canal in the inner and outer zone, and in the middle zone, these fibers arrange circumferentially around the endocervical canal (Fig. 2(b)).[6–8] However, the fibers, which are aligned perpendicularly to the ectocervical surface, cannot be visualized through two-dimensional colposcopic images. It is also very difficult to detect exactly the boundary between these zones. In this research, the ectocervix is separated into two radial zones: Zone 1 includes the inner zone and a small part of the middle zone, and Zone 2 includes the rest of the ectocervix. The collagen fiber orientation distribution and dispersion were presented at four anatomic quadrants (anterior (A), posterior (P), left (L), and right (R) quadrants) in Zone 2 (Fig. 2(c)).

2.3. *Image analysis with orientationJ*

The fiber alignment measurement was characterized by using an ImageJ (Version 1.52a, by Wayne

Table 1. Demographic factors between the different gravidity groups.

	Gravidity			
Demographic factor	0	1	2	3
Number of subjects (24)	6	9	7	2
Percentage of subjects (%)	25%	37.5%	29.17%	8.33%
Mean age	31	31.11	31.43	38.5
Pregnancy Status	NP	NP	NP	NP

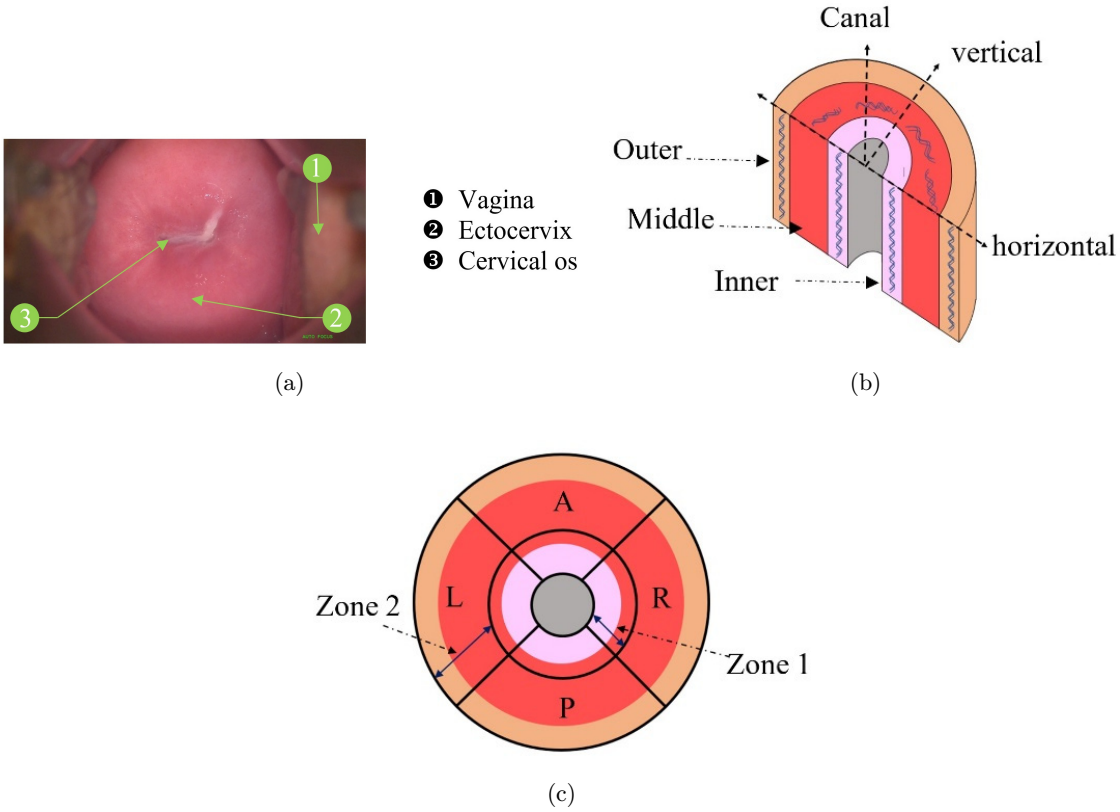

Fig. 2. (a) Polarized RGB image of a normal adult nonpregnant cervix, (b) Three theory zones of the cervical collagen network: inner, middle, and outer zones.[6] (c) Illustration of four anatomical quadrants (A-anterior, P-posterior, L-left, and R-right) in Zones 1 and 2 for fiber orientation and dispersion analysis.

Rasband, National Institutes of Health, USA) plug-in (OrientationJ). OrientationJ uses the first derivative and a Gaussian weighting function to construct a structure tensor with four functionalities: (1) Performing a visual representation of the orientation of an image, (2) creating a vector field map, (3) plotting the distribution of orientations, and (4) detecting of keypoints. It has also been commonly used for measuring the orientation and coherency in a ROI of images. The coherence coefficient, which ranges from 0 to 1, indicates the dispersity of the fiber orientations. Larger values of coherency coefficient correspond to low fiber dispersion, and smaller numbers indicate higher fiber dispersion.[18–20]

Noise, blur, and glare in the image are the major reasons causing problems for automated image analysis systems. Cross-polarization filters can be used to enhance contrast in images as well as eliminate specular reflectance and glare. To show the effectiveness of this technique, Tilapia fish skin was selected as a phantom in our model (Fig. 3), as it has been suggested as an option of biological material for the management of burn wounds as well as a biological graft in gynecology.[21] Two images of the same position of the Tilapia fish skin sample were captured under nonpolarized (NP) light and cross-polarized (CP) light. The image with CPs showed considerably less glare from the surface, thereby improving image contrast and allowing for a more detailed evaluation of underlying structures (Figs. 3(a) and 3(b)). In Figs. 3(c) and 3(d), the results of OrientationJ analysis for determining texture orientation were presented. To understand the difference, we randomly selected three corresponding regions (A, B, and C) located in the same position of each sample to analyze differences between them. We can see that the orientation distribution of the texture is different in the two images. The probability distributions gathered in Figs. 3(e) and 3(f) show that regions A, B, and C have almost the same preferred orientation in the CP mode, while they have been fully randomly arranged in the NP mode. Overall, the Tilapia fish skin sample which was observed using the CP light is consistent with the results of several previous

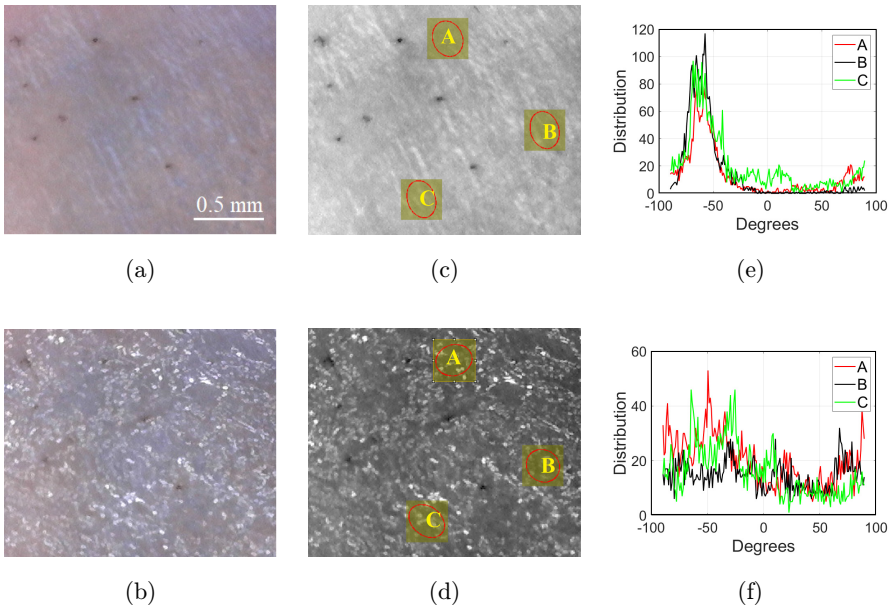

Fig. 3. Distinguishing between images of the Tilapia fish skin samples. (a) With cross-polarization detection (CP mode) and (b) with nonpolarization detection (NP mode). Three corresponding regions (A, B, and C) were shown in the CP mode (c) and NP mode (d). Comparing angular distributions of region A (red solid), region B (black solid), and region C (green solid) in the CP mode (e), and NP mode (f).

studies, where the collagen fibers were well organized and distributed in a parallel pattern.[22] The results were also shown that the angular distribution of the sample was observed using NP light, which cannot be measured exactly by using orientation. It can be concluded that glare is one of the main factors causing deviated results when using OrientationJ to measure automatically the orientations in test samples. Therefore, applying any image processing in the glare region is impossible. On the other hand, many research studies recently have demonstrated that polarized light microscopy is a powerful technique for measuring the properties of the collagen fibers of the biological samples.[23] Therefore, we propose an effect estimation method to determine the collagen fiber orientation distribution and dispersion of the cervix using polarized light colposcopy.

2.4. *Tissue absorption*

The surface color of the cervix is influenced by the absorption spectrum of hemoglobin. Hemoglobin is found in the blood vessels located in the stroma. In this method, cervical images obtained by the CMOS camera were separated into three grayscale images (Red, Green, and Blue channel images). The hemoglobin absorption spectrum exhibits a major peak in the blue light, and a minor one in the green light. Due to the decrease of the absorption by hemoglobin, the light penetration depth also increases with increasing wavelengths from the range of wavelengths from green light to red light. Thus, the Green channel image is characterized by high contrast and contains more information than the Blue channel image. It is commonly used for analyzing blood vessel image data or performing segmentation of blood vessels. The appearance of the blood vessels in the Green and Blue channel looks more contrasted than the background, it will cause the uneven distribution of pixel intensity on the surface of the cervix. However, the OrientationJ based on the evaluation of the gradient structure tensor in a local neighborhood can be used to detect the orientation of objects. Changes in the intensity of an image have a significant effect on the estimation of the directional and organized collagen fibril. In contrast, hemoglobin has significantly lower absorption light in the red than in the other regions of the visible spectrum. This property makes blood vessels appear much lighter than that of the background in the Red channel image. In addition, the absorption of collagen is slightly higher than hemoglobin in the red regions.[16] Therefore, Red channel image could also be used to produce a high contrast image for collagen structures in the cervix. Finally, the red

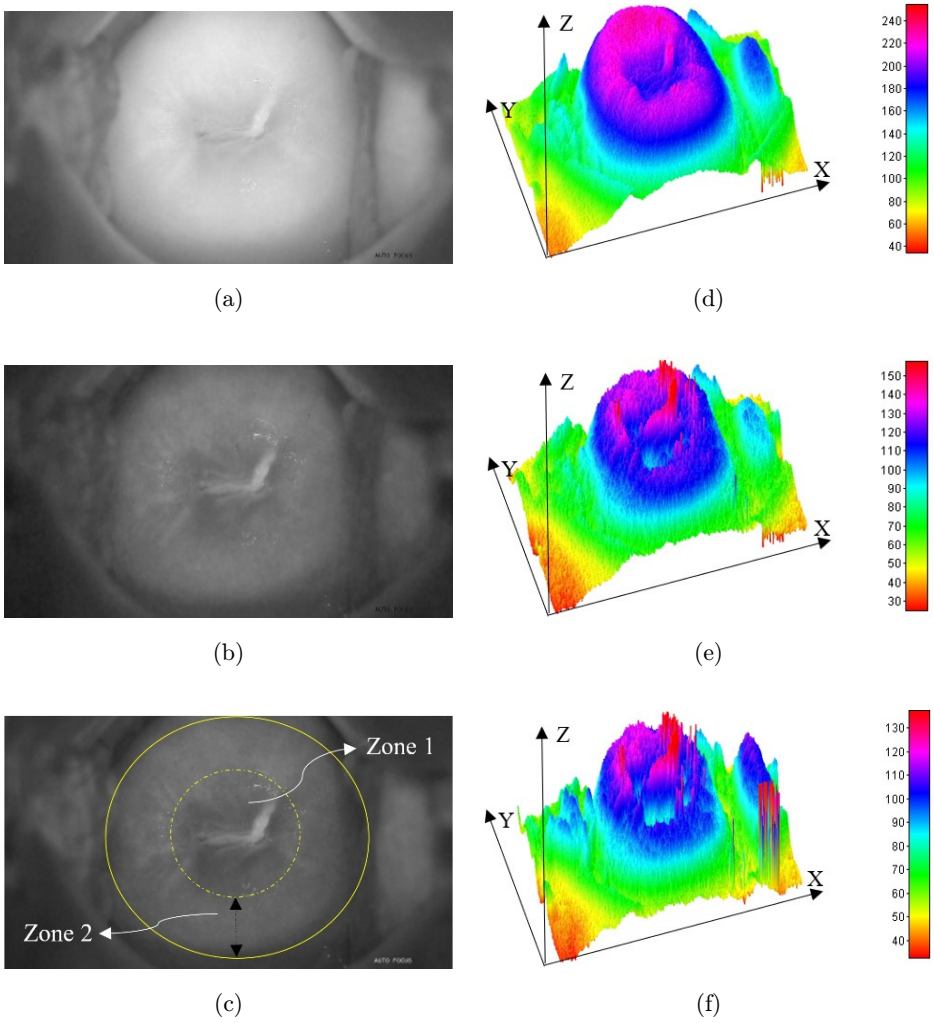

Fig. 4. Red, Green, and Blue channels of a case of a nonpregnant image are shown in Fig. 2. Each channel is depicted as a grayscale image: (a) Red channel, (b) Green channel, (c) Blue channel. 3D contour map comparisons of Red, Green and Blue channels for the same tuples are also provided (d)–(f) respectively.

light penetration into cervical tissue is deeper than the penetration of blue light and green light. For all of these reasons, the Red channel is selected for further operations in the collagen orientation estimation.

A case of a nonpregnant cervix (Fig. 2(a)) was divided into the Red, Green, and Blue channels (Figs. 4(a)–4(c)). We have discussed earlier that the interaction between light and tissue depends on the wavelengths of the incident light. As a result, display information is different among the Red, Green, and Blue channels. For more clearly direct observation of the distribution of pixel intensities, the 3D contour map of cervix surface obtained from Red, Green, and Blue channels were shown in Figs. 4(d)–4(f), respectively. These images show the ability to distinguish the ectocervix region inside the yellow circle (Fig. 4(c)) from the background. As shown in Fig. 4(c), to determine the orientation of collagen fibers, the ectocervix was divided into Zones 1 and 2. From the 3D contour map shown in Figs. 4(e) and 4(f), we can easily recognize that the intensity values of the pixels of Zones 1 and 2 have changed drastically. This sudden change can lead to measurement errors in collagen fibers orientation estimation using OrientationJ. On the other hand, as we can see in Fig. 4(d), the pixel values have been more evenly distributed throughout Zone 1 as well as the Zone 2 of the ectocervix. In brief, the Red channel has a smooth surface with fewer unexpected noises.

3. Results and Discussion

As mentioned above, mapping collagen fiber in the cervical surface is a challenge. By selecting the

cervical image in the Red channel and using the cross-polarized method, influences of blood vessels and surface glare were minimized to an acceptable level. After separating the image of the cervix in the Red channel from the raw image, Red channel image was smoothed with a 3×3 median to remove outlier pixels with a shift in the orientation value. Then, OrientationJ was used to determine the orientation properties of ROI in an image. The local orientation properties are calculated according to the structure tensor created by collagen fiber absorption intensity and visualized as color images with the orientation encoded in a hue saturation-brightness map where hue is orientation, saturation is coherency, and brightness is the same as the original image. To facilitate calculating collagen alignment, collagen fibers orientation is represented by a vector field, called collagen fibers orientation map. Each vector has the same dimension with collagen fibers in a 50×50 pixels sub-region.

Figure 5 shows the example of the directionality maps using OrientationJ of nonpregnant cervix live sample (Fig. 2(a)). The Red, Green, and Blue channels of the color image were used as input of the structure tensor computation. For visualizing the existence of distinct fiber distribution groups at different orientations, collagen fiber orientation distribution was presented by an HSB color-coded map. Each color represents an angle of the segment $[-90°, 90°]$. As mentioned above, the ectocervix was divided into two radial zones. We can see that the Red channel extraction makes the distribution map of collagen fiber orientation is different in these zones more clearly (Fig. 5(a)). Zone 1 has turbulence distribution of the colors whereas Zone 2 has symmetry distribution across the cervical OS.

This means that cervical collagen fibers have the circumferential trend in Zone 2 and random distribution in Zone 1. However, similar distribution trends of orientation are not observed in the Green and Blue channel images (Figs. 5(b) and 5(c)). This proves once again that the Red channel provides the best view for collagen fiber orientations in cervical tissues compared to the other two channels.

Collagen fibers orientation maps of cervix live samples were presented by vector field using OrientationJ (Fig. 6). Each vector stands for collagen alignment in about 50×50 pixels sub-region. The orange bars show local fibers orientation in each sub-region. For studying collagen fibers orientation distribution in Zone 2, four quadrants were selected to compare: Anterior (A), posterior (P), left (L), and right region (R). The normalized angular distributions of each quadrant region were shown in Fig. 6. We can see that the OrientationJ analysis detects the presence of fibers at $0°$ in anterior and posterior regions. Whereas, OrientationJ analysis produces strong peaks at $90°/-90°$ for both left and right regions. The angular distribution analyses of each quadrant region are similar in all other cervical samples.

We compared the histograms of the fiber metrics at all four quadrants (A, P, L, R) regions for both Zones 1 and 2. The significant difference occurred in fiber orientation, which is found in Figs. 7(a)–7(d). The graphs describe this situation in detail, where for Zone 2, the orientation angle of most fibers is close to $0°$ (A, P region) and $90°/-90°$ (L, R region), indicating fibers are more likely aligning along a certain direction, whereas for Zone 1, the fiber orientation seemed to be more random at all four quadrants (A, P, L, R) region. To further confirm the alignment and provide an angle distribution map in the horizontal plane of the cervix, we split the four quadrants regions into small sub-regions and calculated the angle in each sub-region. A total of 60 sub-regions were selected around Zone 2, and 48 sub-regions around Zone 1. The orientation angle

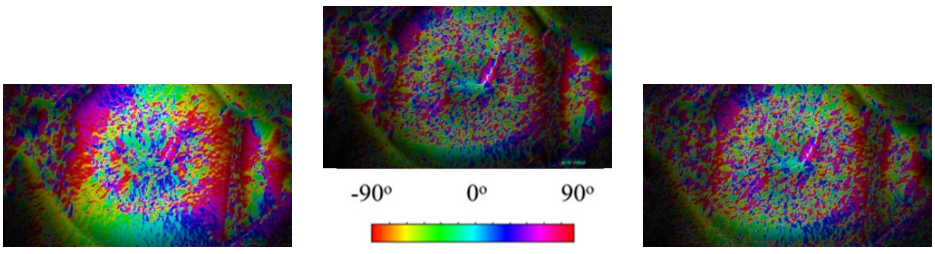

(a) (b) (c)

Fig. 5. Collagen fiber visualization map of a nonpregnant sample (in Fig. 2(a)) of Red channel image (a), Green channel image (b), and Blue channel image (c) using OrientationJ. The color bar corresponds to dominant fiber orientation on the ectocervix $[-90°, 90°]$.

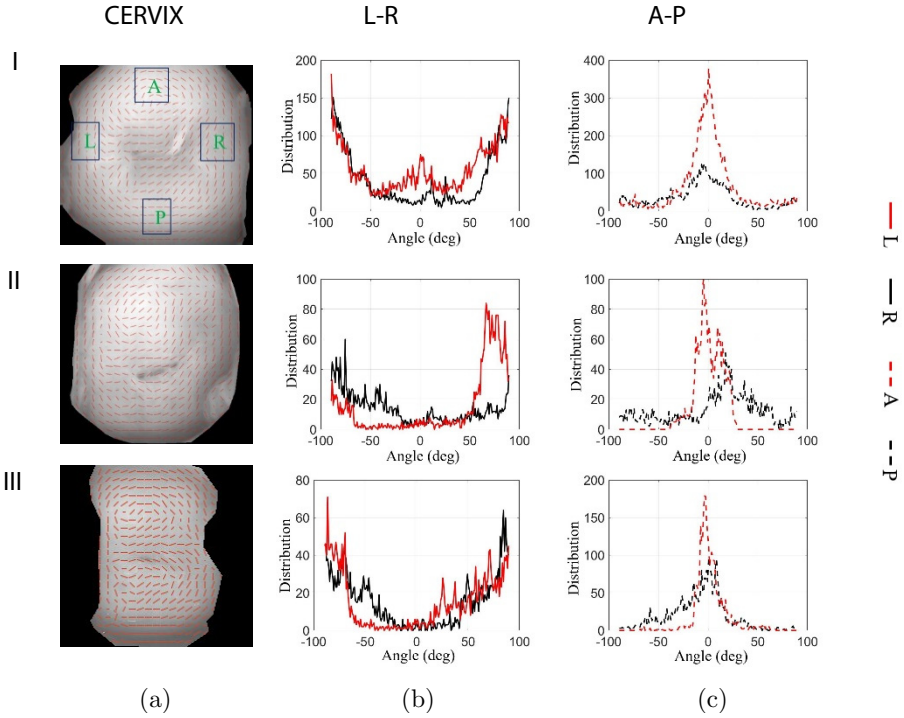

Fig. 6. (a) Collagen fibers orientation maps in Zone 2 of three nonpregnant samples are presented by vector field using OrientationJ. (b) Comparing angular distributions of the anterior region (red dotted) and posterior region (black dotted). (c) Comparing angular distributions of the left region (red solid) and right region (black solid).

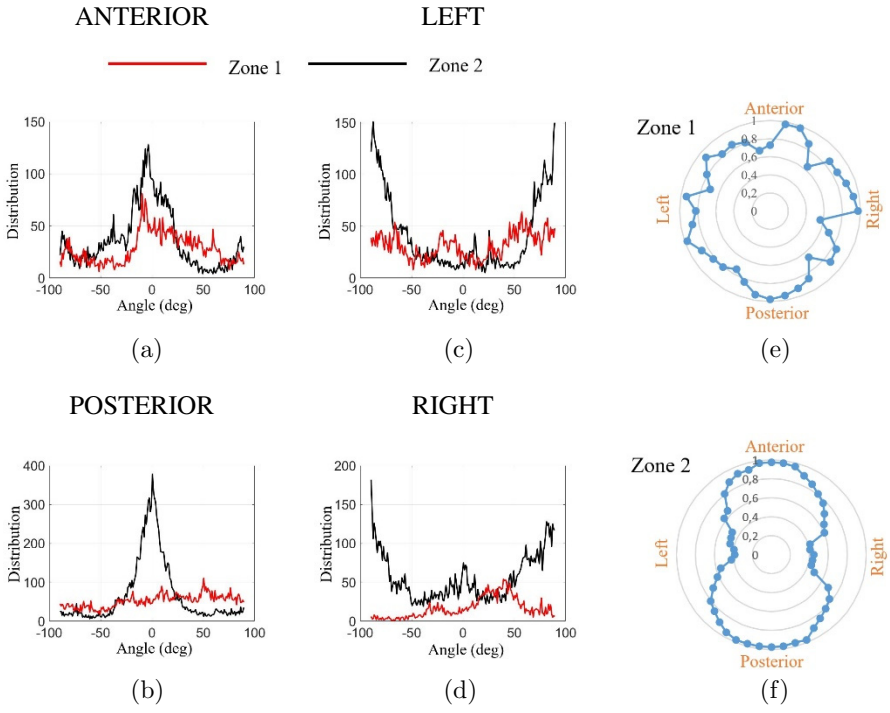

Fig. 7. Comparison of the angle distribution at all four quadrants region corresponding to the Red channel image of sample 1 (shown in Fig. 4(a)). The pairs of histograms in (a) anterior, (b) posterior, (c) left, and (d) right. The orientation angle of each sub-region was shown on the polar diagram with (e) Zone 1 and (f) Zone 2.

of each sub-region is shown on the polar diagram (Figs. 7 (e) and 7(f))). The radius R (arbitrary unit) is calculated by the formula (1), where $\theta \in [0, 2\pi]$ is the orientation angle of each sub-region.

$$R = 0.375 + 0.625 \times |\cos(\theta)|. \quad (1)$$

As we can see, the orientation of collagen fibers is randomly oriented in Zone 1 (Fig. 7(e)), and circumferential trends in Zone 2 (Fig. 7(f)).

The changes in collagen alignment have an extremely important role in the mechanical properties, physiological, and biochemical functions of cervical tissues. The dispersity of collagen fiber orientation can be estimated by a statistical measure called the alignment coefficient. There are several types of alignment coefficients, such as anisotropy index based on eigenvalues of a second rank tensor, anisotropy based on the circular variance in circular statistics, and coherency based on the ratio between the difference and the sum of the eigenvalues.[18,19]

In this research, the coherency coefficient was used to indicate the dispersity of the fiber orientations. The values range between 0 and 1. Here 1 indicates perfectly aligned fibers (correspond to low fiber dispersion) and smaller values represent more randomly distributed fibers (correspond to strong fiber dispersion). To further analyze the dispersion of fiber organization, the coherency coefficient corresponding to fiber dispersion is computed at all four quadrants (A, P, L, R) from all 24 cervical samples in both Zones 1 and 2. The coherency coefficient of all samples is shown in Fig. 8. The results indicated that the values of the coherency coefficient were region-dependent in the ectocervix. When choosing 50×50 pixels sub-regions in Zone 1, the values of the coherency coefficient are very low at all four quadrants region in Zone 1 (mean = 0.06) (Fig. 8(a)). This means that fiber orientation tended more randomly along the radial direction, and the collagen fibers are much more heterogeneous distributed. In contrast, the values of the coherency coefficient in Zone 2 (mean = 0.3) are nearly five times higher than that in Zone 1 (Fig. 8(b)). These trends show that fiber orientation tended in Zone 2 more preferentially aligned, and the collagen fibers are more homogeneous spatial distribution. When comparing 50×50 pixels sub-regions at four quadrants region in Zone 2, the values of the coherency coefficient are higher in the posterior (0.350 ± 0.095) and left (0.313 ± 0.079) quadrants compared to that in anterior (0.254 ± 0.050) and right (0.275 ± 0.082) quadrants (Fig. 8(b)).

In this paper, we introduced a new method, which can be used in practice to measure cervical collagen orientation and dispersion as well as to conduct a feasibility study on human cervical tissue ($n = 24$). This method can be applied in three main steps: (1) Polarization adapter is attached to a colposcope for capturing orthogonally polarized images to eliminate glares and specular highlights as well as get more information deeper into the tissue volume; (2) the Red channel which has a smooth surface with fewer unexpected noises is selected for further operations in the collagen orientation estimation method; (3) Orientaion J analysis is used to objectively quantify collagen morphology.

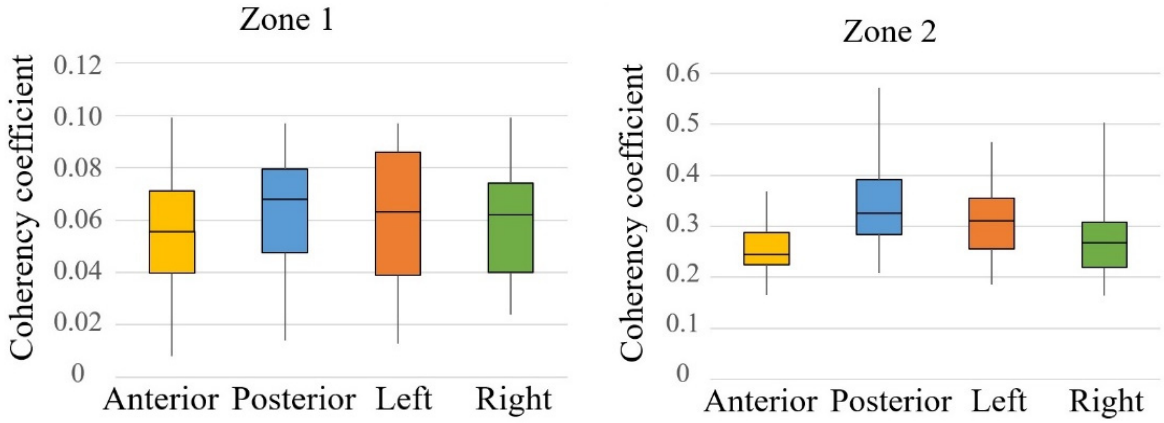

(a) (b)

Fig. 8. Coherency analysis at all four quadrants region in Zone 1 (a) and Zone 2 (b).

We carefully compared our results with similar papers, which used X-ray, SHG, OCT, and MMP to study the characterization of cervical collagen in nonpregnant women *in vivo* and *in vitro*. These studies proved that the cervical collagen network in the ECM consists of three anatomic zones with distinct collagen fibers orientation. In the inner and outer zone, collagen fibers are arranged parallel to the canal. In the middle zone, the collagen fibers have a preferred orientation in a circumferential around the canal.[6–11] Unlike X-ray, SHG, and OCT that can produce in-depth image-specific cross-sections below the surface of the cervix, the polarized colposcopic images are 2D whole field images of the ectocervix. With our 2D images, it is very difficult to detect exactly the boundary of the collagen fibrils distribution. Besides that, during the colposcopy, if the speculum is not too widely separated, the outer zone of the ectocervix may be hidden by the walls of the vagina. Therefore, we separated the ectocervix into two radial zones: Zone 1 includes the inner zone and a small part of the middle zone, and Zone 2 includes the rest of the ectocervix, this is similar to that observed by Yao *et al.*[8] First, we found that Zone 2 has circumferentially aligned fibers while Zone 1 was randomly arranged. The collagen fiber dispersion in Zone 2 is much smaller than that in Zone 1. This is achieved through similar results in Refs. 6–11. Second, for nonpregnant samples, OCT images show that the posterior and anterior quadrants of the outer zone had more aligned fibers compared to the left and right quadrants,[8] while by the SHG ellipticity measurement, the collagen fibers have a similar degree of alignment at all four quadrants region.[9] In our study, the left and posterior quadrants are more aligned than the other anatomic zones.

There are several limitations in the methods of this work. The images presented in this work are 2D field images of the cervix. Using the 2D data does not help us recognize any differences in the orientation of collagen fibers in deeper layers of the cervix. It is best suited to investigate the changes in collagen circumferentially aligned around the cervix os. In addition, only nonpregnant cervical samples were obtained. In this study, the imaging was accepted in healthy or inflammatory of the cervix. Ectopy, polyp, cervical dysplasia, pre-invasive cervical disease, cervical intraepithelial neoplasia, etc., were eliminated before starting the analysis. Further research on collagen orientation in cervical remodeling is needed to evaluate the effectiveness of this work.

4. Conclusions

The ECM is a dense network of collagen fibers, which is the load-bearing component of the cervical tissue. Identification of cervical microstructural architecture during specific stages of the cervix is necessary for the study of cervical diseases and giving suitable treatments in time. In this paper, a new method was presented for quantitative fiber orientation analysis and visualization within the cervix *in vivo*. We found that in the nonpregnant cervix, Zone 2 (middle zone) has circumferentially aligned collagen fibers that are less dispersed than Zone 1 (inner zone) at all four quadrants region. This result is consistent with the previous studies. In further studies, collagen fiber orientation in the pregnant cervix will be analyzed for understanding the changing of collagen fiber direction trends. In summary, this method is simple, fast, low-cost, and effective for measuring changes in cervical collagen fibers orientation, which could be applied to diagnosis in providing a quantitative platform for the clinical environment.

Conflicts of Interest

The authors declare that there are no conflicts of interest regarding the publication of this article.

Acknowledgments

We acknowledge the support of time and facilities from Ho Chi Minh City University of Technology (HCMUT), VNU-HCM for this study.

This research was supported by the Ho Chi Minh City Department of Science and Technology of Vietnam, under grant number 116/2020/HD-QPTKHCN.

References

1. R. A. Word, X. H. Li, M. Hnat, K. Carrick, "Dynamics of cervical remodeling during pregnancy and parturition: mechanisms and current concepts," *Semin. Reprod. Med.* **25**(1), 69–79 (2007).
2. K. M. Myers, H. Feltovich, E. Mazza, J. Vink, M. Bajka, R. J. Wapner, T. J. Hall, M. House, "The

mechanical role of the cervix in pregnancy," *J. Biomech.* **48**(9), 1511–1523 (2015).
3. R. Holt, B. C. Timmons, Y. Akgul, M. L. Akins, M. Mahendroo, "The molecular mechanisms of cervical ripening differ between term and preterm birth," *Endocrinology* **152**(3), 1036–1046 (2011).
4. S. Xu, H. Xu, W. Wang, S. Li, H. Li, T. Li, W. Zhang, X. Yu, L. Liu, "The role of collagen in cancer: From bench to bedside," *J. Translational Med.* **17**(1), 309 (2019).
5. W. Prendiville, R. Sankaranarayanan, Colposcopy and Treatment of Cervical Precancer, *IARC Technical Publication No. 45, Lyon (FR): International Agency for Research on Cancer*, pp. 13–21 (2017).
6. R. M. Aspden, "Collagen Organisation in the Cervix and its Relation to Mechanical Function," *Collagen Rel. Res.* **8**(2), 103–112 (1988).
7. Y. Gan, W. Yao, K. M. Myers, J. Y. Vink, R. J. Wapner, C. P. Hendon, "Analyzing three-dimensional ultrastructure of human cervical tissue using optical coherence tomography," *Biomed. Opt. Exp.* **6**(4), 1090–1108 (2015).
8. W. Yao, Y. Gan, K. M. Myers, J. Y. Vink, R. J. Wapner, C. P. Hendon, "Collagen fiber orientation and dispersion in the upper cervix of non-pregnant and pregnant women," *PloS One* **11**(11), e0166709 (2016).
9. J. Hao, W. Yao, W. B. R. Harris, J. Y. Vink, K. M. Myers, E. Donnelly, "Characterization of the collagen microstructural organization of human cervical tissue," *Reproduction* **156**(1), 71–79 (2018).
10. L. M. Reusch, H. Feltovich, L. C. Carlson, G. Hall, P. J. Campagnola, K. W. Eliceiri, T. J. Hall, "Nonlinear optical microscopy and ultrasound imaging of human cervical structure," *J. Biomed. Opt.* **18**(3), 031110 (2013).
11. J. Chue-Sang, N. Holness, M. Gonzalez, J. Greaves, I. Saytashev, S. Stoff, A. Gandjbakhche, V. Chernomordik, G. Burkett, J. Ramella-Roman, "Use of Mueller matrix colposcopy in the characterization of cervical collagen anisotropy," *J. Biomed. Opt.* **23**(12), 1–9 (2018).
12. P. Shukla, A. Pradhan, "Mueller decomposition images for cervical tissue: Potential for discriminating normal and dysplastic states," *Opt. Exp.* **17**(3), 1600–1609 (2009).
13. J. Vizet, J. Rehbinder, S. Deby, S. Roussel, A. Nazac, R. Soufan, C. Genestie, C. Haie-Meder, H. Fernandez, F. Moreau, A. Pierangelo, "*In vivo* imaging of uterine cervix with a Mueller polarimetric colposcope," *Sci. Rep.* **7**, 2471 (2017).
14. M. Gonzalez, K. A. Montejo, K. Krupp, V. Srinivas, E. DeHoog, P. Madhivanan, J. C. Ramella-Roman, "Design and implementation of a portable colposcope Mueller matrix polarimeter," *J. Biomed. Opt.* **25**(11), 116006 (2020).
15. D. G. Ferris, W. Li, U. Gustafsson, R. W. Lieberman, O. Galdos, C. Santos, "Enhancing colposcopy with polarized light," *J. Low. Genit. Tract Dis.* **14**(3), 149–154 (2010).
16. T. V. Tien, N. N. Quynh, L. H. Duc, P. N. K. Cat, H. Q. Linh, "Detection and localization of the hemoglobin and collagen distribution of the uterine cervix," *J. Innov. Opt. Health Sci.* **12**(4), 1942006 (2019).
17. S. Holmen, H. N. Galappaththi-Arachchige, E. Kleppa, P. Pillay, T. Naicker, M. Taylor, M. Onsrud, E. F. Kjetland, F. Albregtsen, "Characteristics of blood vessels in female genital schistosomiasis: Paving the way for objective diagnostics at the point of care," *PLOS Neglected Trop. Dis.* **10**(4), e0004628 (2016).
18. Y. Liu, A. Keikhosravi, G. S. Mehta, C. R. Drifka, K. W. Eliceiri, "Methods for quantifying fibrillar collagen alignment," *Meth. Mol. Biol.* **1627**, 429–451 (2017).
19. T. Clemons, M. Bradshaw, P. Toshniwal, N. Chaudhari, A. Stevenson, J. Lynch, M. W. Fear, F. M. Wood and K. S. Iyer, "Coherency image analysis to quantify collagen architecture: implications in scar assessment," *RSC Adv.* **8**(18), 9661–9669 (2018).
20. R. Rezakhaniha, A. Agianniotis, J. T. C. Schrauwen, A. Griffa, D. Sage, C. V. C. Bouten, F. N. van de Vosse, M. Unser, N. Stergiopulos, "Experimental investigation of collagen waviness and orientation in the arterial adventitia using confocal laser scanning microscopy," *Biomech. Model. Mechanobiol.* **11**(3–4), 461–473 (2012).
21. E. M. Lima-Junior, M. O. de Moraes Filho, B. A. Costa, F. V. Fechine, M. E. A. de Moraes, F. R. Silva-Junior, M. F. A. N. Soares, M. B. S. Rocha, C. M. P. Leontsinis, "Innovative treatment using tilapia skin as a xenograft for partial thickness burns after a gunpowder explosion," *J. Surg. Case Rep.* **2019**(6), rjz181 (2019).
22. M. T. P. M. Dias, E. M. L. Júnior, A. P. N. N. Alves, A. P. M. Bilhar, L. C. Rios, B. A. Costa, E. S. R. Matos, A. C. Venancio, Z. V. Bruno, M. O. M. Filho, L. R. P. S. Bezerra, "Tilapia fish skin as a new biologic graft for neovaginoplasty in Mayer-Rokitansky–Kuster–Hauser syndrome: A video case report," *Fertil. Steril.* **112**(1), 174–176 (2019).
23. A. P. N. N. Alves, E. M. L. Júnior, N. S. Piccolo, M. J. B. Miranda, M. E. Q. L. Verde, A. E. C. F. Júnior, P. G. B. Silva, V. P. Feitosa, T. J. P. G. de Bandeira, M. B. Mathor, M. O. de Moraes, "Study of tensiometric properties, microbiological and collagen content in nile tilapia skin submitted to different sterilization methods," *Cell and Tissue Bank.* **19**(3), 373–382 (2018).